J. Fluid Mech. (1968), *vol.* 34, *part* 4, *pp.* 625–639
Printed in Great Britain

Distribution of local pressure and skin friction around a circular cylinder in cross-flow up to $Re = 5 \times 10^6$

By E. ACHENBACH
Institut für Reaktorbauelemente, KFA-Jülich, Germany

(Received 15 March 1968)

In a large range of Reynolds numbers, $6 \times 10^4 < Re < 5 \times 10^6$, the flow around single cylinders with smooth surfaces has been investigated. The high values of the Reynolds numbers were obtained in a test channel which could be pressurized up to 40 bar of static pressure. New experiments were performed to measure the local pressure and skin friction distribution around the cylinder. From these results the total drag, the pressure drag and the friction drag were calculated. By means of the skin friction distribution the position of the separation points, separation bubbles or transition points can be localized. These data allow one to define three states of the flow: the subcritical flow, where the boundary layer separates laminarly; the critical flow, in which a separation bubble, followed by a turbulent reattachment, occurs; and the supercritical flow, where an immediate transition from the laminar to the turbulent boundary layer is observed at a critical distance from the stagnation point. According to the total drag coefficient the values found in this paper connect the subcritical region represented by the measurements of Wieselsberger (1923) and Fage & Warsap (1930) with the supercritical range in which Roshko (1961) carried out his experiments.

1. Introduction

Investigations on tube banks in cross-flow have shown that, beginning at a critical Reynolds number, an improvement of heat transfer in connexion with the increase of the pressure-drop coefficient is to be observed. This change is rather important so it must be taken into account when designing heat exchangers for extremely high Reynolds numbers. In order to get a deeper insight into these phenomena, we started investigations on heat transfer and flow mechanism. In this paper those preliminary experiments are communicated which have been made with a single cylinder in cross-flow with a smooth surface. In a region of $6 \times 10^4 < Re < 5 \times 10^6$ the distribution of the local pressure and skin friction has been measured around the cylinder. With these values available, the total drag, the pressure drag and the friction drag could be calculated. Finally we found the position of the separation point as a function of the Reynolds number.

2. Experimental arrangement

The investigations were performed in two test rigs which were available in the 'Institut für Reaktorbauelemente, Kernforschungsanlage Jülich'. The fluid was air. The atmospherical tests were carried out in the low-pressure wind tunnel (ND channel). The tests carried out up to 40 bar static pressure were conducted in the pressurized wind tunnel (HD channel). The rectangular test section (500 × 900 mm) could be mounted alternatively in the ND channel or in the HD channel. Table 1 gives some technical data. A detailed description of the test rigs has been published by Grosse & Scholz (1965, pp. 150–8).

Channel	Pressure (bar)	Temperature (°C)	Velocity$_{max}$ (m/s)	Re_{max}	Mach number	Tu (%)
ND	1	60	35	3×10^5	< 0·1	0·7
HD	1–40	60	15	$4{\cdot}7 \times 10^6$	< 0·05	

TABLE 1. Experimental data of the test channels

The test cylinder was a brass tube with a length of $L = 500$ mm and a diameter $d = 150$ mm. The maximum deviation of the tube diameter was 0·15 mm. For control another cylinder 1000 mm in length was used. The surfaces of the tubes were polished. The total height of the roughness was 2μm, measured in the axial direction. Before starting the experiments the flow conditions were calibrated. The velocity profile in the test section was nearly plane within the range of $\pm 1\,\%$ of the mean value.

The turbulence level

$$Tu = \frac{\sqrt{(\overline{u'^2})}}{U_\infty},$$

where u' is the velocity fluctuation and U_∞, the undisturbed velocity, was measured with a hot wire. The obtained value was $Tu = 0{\cdot}7\,\%$. The temperature of the fluid was controlled at a value of nearly 60 °C. The deviation of the blower rotation was kept in the range of $\pm 0{\cdot}2\,\%$.

3. Measurement techniques

The velocity at the entrance of the test section U_∞ was calculated from the mass flow, measured by means of a calibrated Venturi nozzle. The accuracy was about 1 %. The calculated velocity was checked by a Prandtl tube. The agreement was very good. The static pressure around the cylinder was measured by means of a pressure hole (1 mm of diameter). It was found nearly at the half length of the cylinder. At the same generator the skin friction probe, described later on, was installed. The pressure hole and the skin friction probe were 10 mm apart. For control another pressure hole was drilled at a distance of 30 mm (detailed construction see figure 1).

The cylinder could be turned around its longitudinal axis from $\phi = 0°$ (stagnation point) to $\phi = 360°$. Thus the static pressure and the skin friction

could be measured simultaneously. At the ND channel the pressure was measured by a Betz manometer. At the HD channel a set of five electronic pressure transducers of various ranges was used. The accuracy was 0·5 % of the full deflexion.

For the dimensionless presentation of the local static pressure the term

$$P = \frac{p - p_\infty}{(\frac{1}{2}\rho) U_\infty^2}$$

was used. $p = p(\phi)$ is the static pressure at the peripherical angle ϕ of the cylinder and p_∞ the static pressure of the infinite flow.

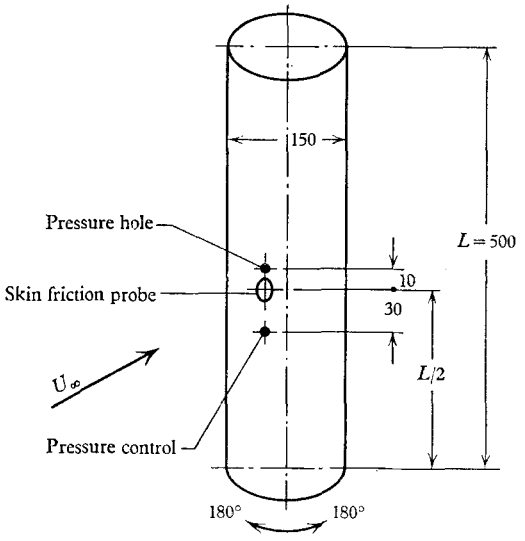

FIGURE 1. Test cylinder (scheme).

The local shear stresses at the wall were picked up by means of a skin friction probe (figure 2). The application of this type of probe was communicated by Konstantinov & Dragnysh (1955). In Rechenberg's (1962, 1963) experiments, carried out in turbulent boundary layers, the reliability of the probe was confirmed. The principle is based on the measurement of the pressure difference at an edge which transversely projects only some hundredths of a millimetre into the boundary layer. The quantity of the pressure difference Δp only depends on the wall-shear stresses τ_0. The advantage of this probe, compared with other ones, is the change of the sign in the reading out, when the flow changes direction. This fact is important for measurements around the total circumference of the cylinder and for localizing a recirculation. Above all it is possible to work in extremely thin boundary layers, because the edge can be ground off as it becomes necessary.

The procedure of the calibration must be regarded as a disadvantage. Because of the very small size of the probe the surroundings of it must not be changed. This means that the probe has to be calibrated while being mounted. In our case the calibration curve was obtained in the following way: the local

skin friction was calculated in the surroundings of the stagnation point from the distribution of the pressure around the cylinder. The procedure used was that of the so-called 'Blasius Reihe' (see Schlichting 1955). The values of τ_0 aud Δp have been brought into the following relationship:

$$\frac{\Delta p}{\tau_0} = f\left(\frac{\Delta p h^2 \rho}{\eta^2}\right).$$

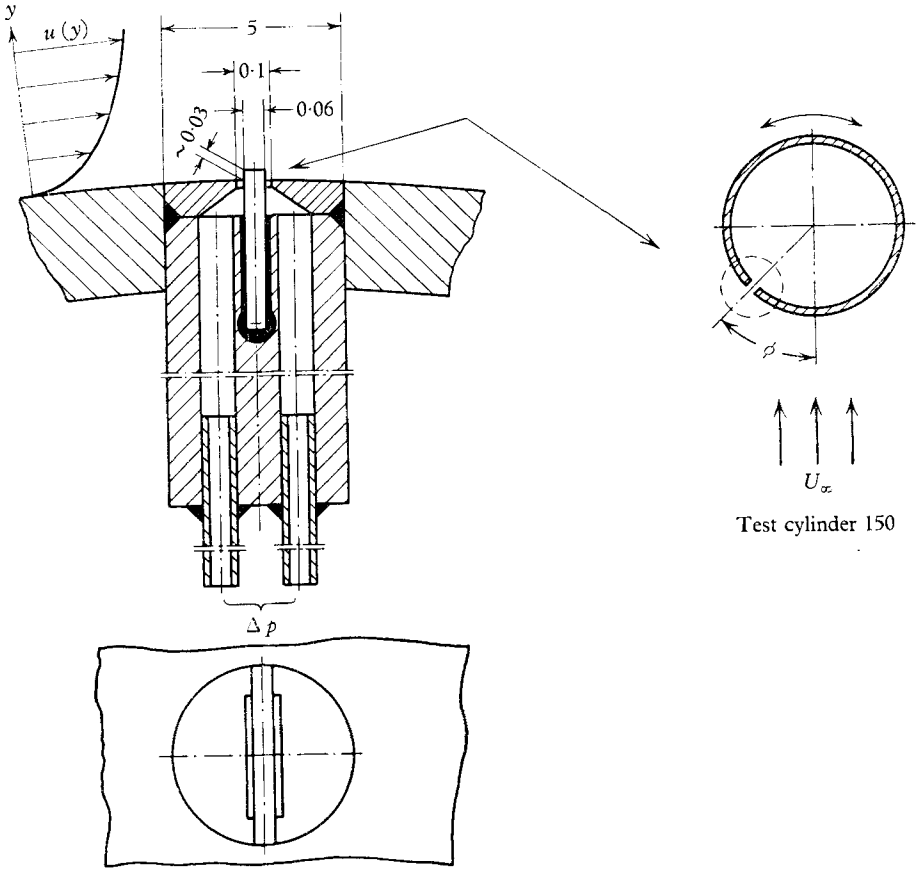

FIGURE 2. Skin friction probe, dimensions in mm.

This equation is obtained by a dimensional analysis, as it is done by Rechenberg (1962) for a test body in a boundary layer. η is the viscosity of the fluid. The term h has the dimension of a length. We ought to introduce h as the height of the edge. In our case, however, the calibration curve must be available for only one height of the probe edge. Therefore an exact measurement of h was not necessary. The calibration curve was picked up for both directions of the flow and for the pressure range of 1 to 40 bar. There is only one line for the entire range, if one takes the calculated values of the skin friction in the region of nearly $0° < \phi < 45°$.

The small pressure differences obtained from the skin friction probe could be measured by means of a fused quartz precision pressure gauge (Texas Instru-

ments, Houston, Texas, U.S.A.). This manometer based on the deflexion of a Bourdon tube even works up to large values of static pressure with a high resolution.

For the presentation of the experimental skin friction the dimensionless term

$$T = \frac{\tau_0}{\rho U_\infty^2}\sqrt{Re}$$

was used, which results in this form from the boundary-layer calculation.

4. Results

4.1. *Pressure and skin friction distribution*

The distribution of the local pressure and skin friction was measured in steps of $\phi = 5°$ around the circumference of $\phi = 360°$ of the cylinder. When necessary the step width was diminished.

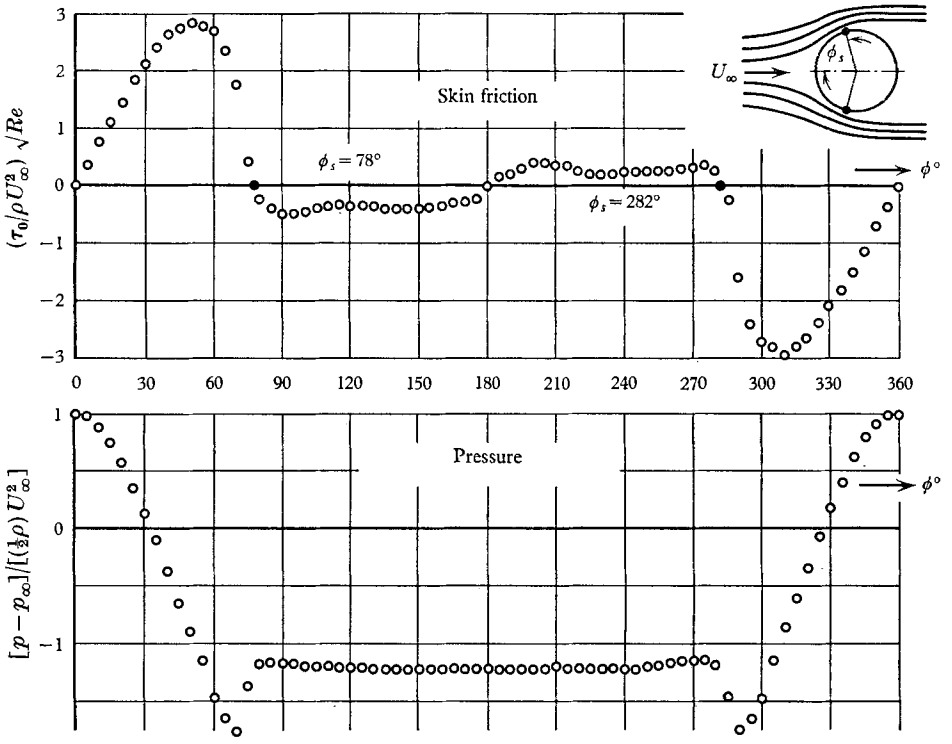

FIGURE 3. Circular cylinder: skin friction and pressure distribution. $Re = 10^5$.

In the four figures 3–6 the skin friction and the corresponding pressure distributions are plotted versus the peripheric angle ϕ of the cylinder.†

Figure 3 shows the case of the subcritical flow at $Re = 10^5$. The boundary layer separates laminarly at $\phi = 78°$ ($\phi = 282°$) before reaching the main cross-

† Details of the numerical measurements are available on request from the editorial office.

section. The separation is indicated by the vanishing of the skin friction. If $\tau_0 = 0$, the velocity gradient at the wall

$$\left(\frac{\partial u}{\partial y}\right)_{y=0} = 0.$$

This is the condition for the separation of the boundary layer from the wall.

Figure 4 shows the behaviour of the flow at $Re = 2{\cdot}6 \times 10^5$. The flow is just before the transition into the critical region which begins at $Re = 3 \times 10^5$. The boundary layer still separates laminarly at an angle of $\phi = 94°$ ($\phi = 266°$).

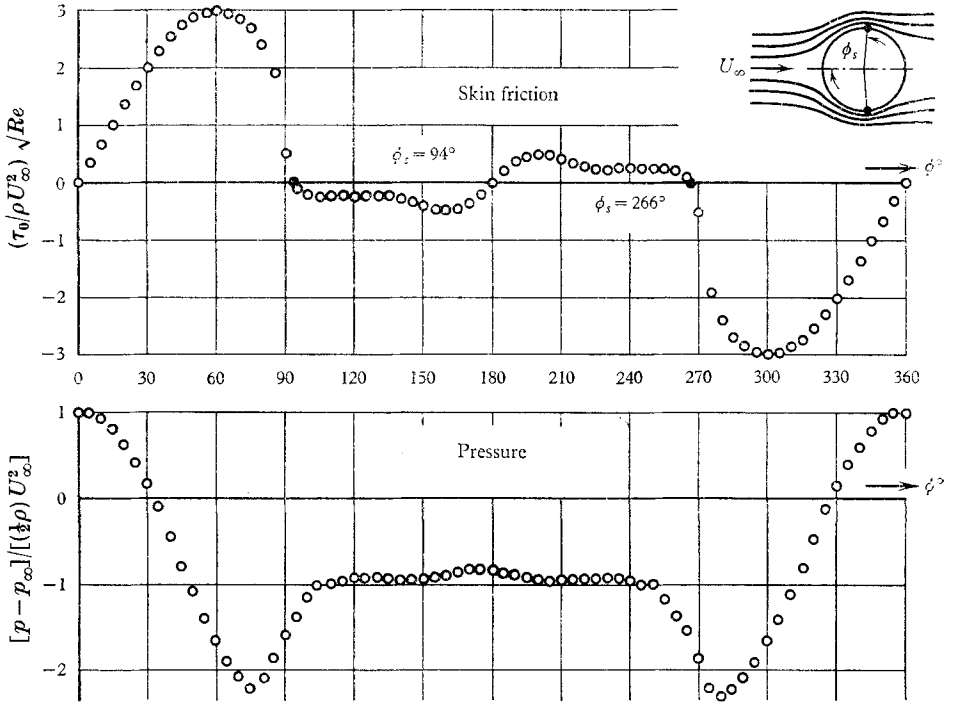

FIGURE 4. Circular cylinder: skin friction and pressure distribution. $Re = 2{\cdot}6 \times 10^5$.

The minimum of the pressure has changed with respect to the magnitude and the position compared with the flow at $Re = 10^5$. The dimensionless pressure in the back of the cylinder rises; this means a decrease of the drag coefficient.

Figure 5 shows the typical distribution of the skin friction which occurs in the critical region. At $\phi = 105°$ ($\phi = 255°$) there is no final separation, but a so-called separation bubble. This means that there is a region between laminar separation and turbulent reattachment in which the wall shear stresses theoretically vanish. Downstream an intensive rise of the skin friction follows, showing values which are mostly greater than those of the laminar maximum. It may be concluded that the boundary layer is now turbulent. At an angle of $\phi = 147°$ ($\phi = 220°$) it separates finally.

Also the pressure distribution confirms that the flow follows the shape of the wall up to $\phi = 147°$ ($\phi = 220°$). The measured distribution comes close to the values of the potential theory in a large range of angle.

This region of Reynolds number characterized by the described behaviour may be called the critical state of the flow. In our measurements it covers the range $3 \times 10^5 < Re < 1{\cdot}5 \times 10^6$. $Re = 3 \times 10^5$ is called the critical Reynolds number. The critical flow is extremely sensitive. Both turbulence level and surface roughness have a significant influence on the flow. This can be recognized by comparing the drag coefficient curves of several authors (figure 9). The critical Reynolds number varies from 2×10^5 to 5×10^5, depending on the special flow conditions.

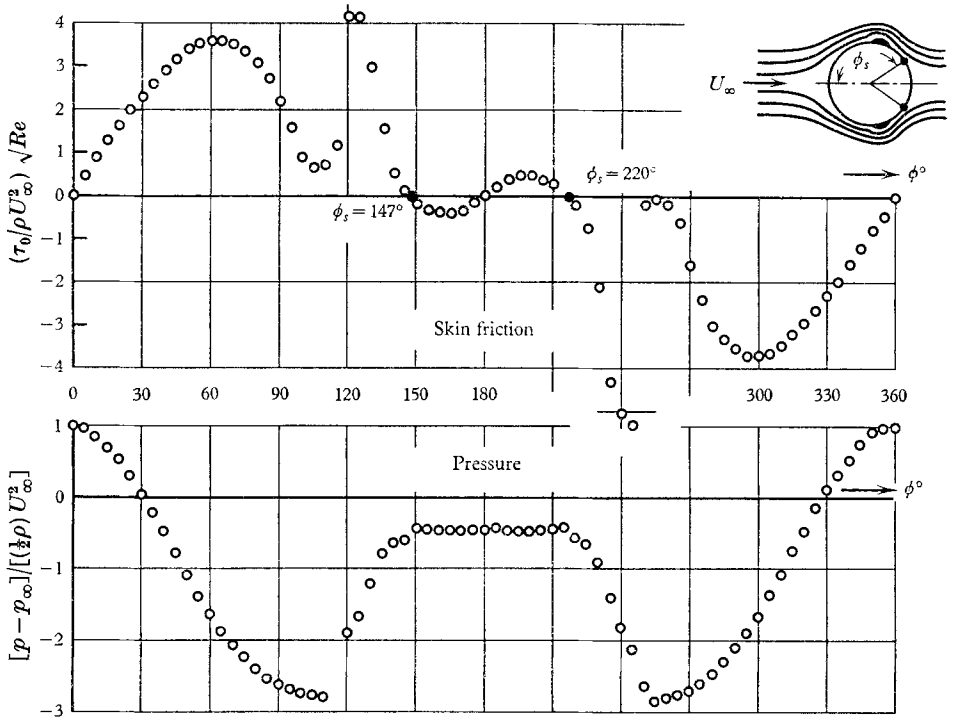

FIGURE 5. Circular cylinder: skin friction and pressure distribution. $Re = 8{\cdot}5 \times 10^5$.

In the region of Reynolds number greater than $1{\cdot}5 \times 10^6$ the phenomenon of the separation bubble is no longer observed. The boundary layer changes without any intermediate state from the laminar to the turbulent flow having reached a critical distance from the stagnation point. The supercritical state of the flow is developed. The position of the transition point is indicated by a small rise and a following retarded drop of the skin friction distribution. The transition point shifts in the direction of the stagnation point if the Reynolds number is increased. In figure 6 it can be localized near $\phi = 65°$ ($\phi = 295°$). Downstream the boundary layer is turbulent. Due to the higher level of energy the turbulent boundary layer is able to run against a pressure gradient from about $\phi = 85°$ to $\phi = 115°$ (from $\phi = 275°$ to $\phi = 245°$).

In order to demonstrate the dependence of the pressure and skin friction distribution upon the Reynolds number, the results just discussed are combined in one diagram (figure 7). In the frontal part of the cylinder the normalized

pressure and skin friction distributions are nearly independent of the Reynolds number. Important changes, however, are found in the rear as was to be expected. In particular, the pressure distribution in the back of the cylinder causes the variation of the drag coefficient presented in figure 9.

The distribution of the static pressure in the subcritical range and in the lower range of the critical flow state has been measured by many authors in former times. However, the flow conditions, above all the turbulence level and the

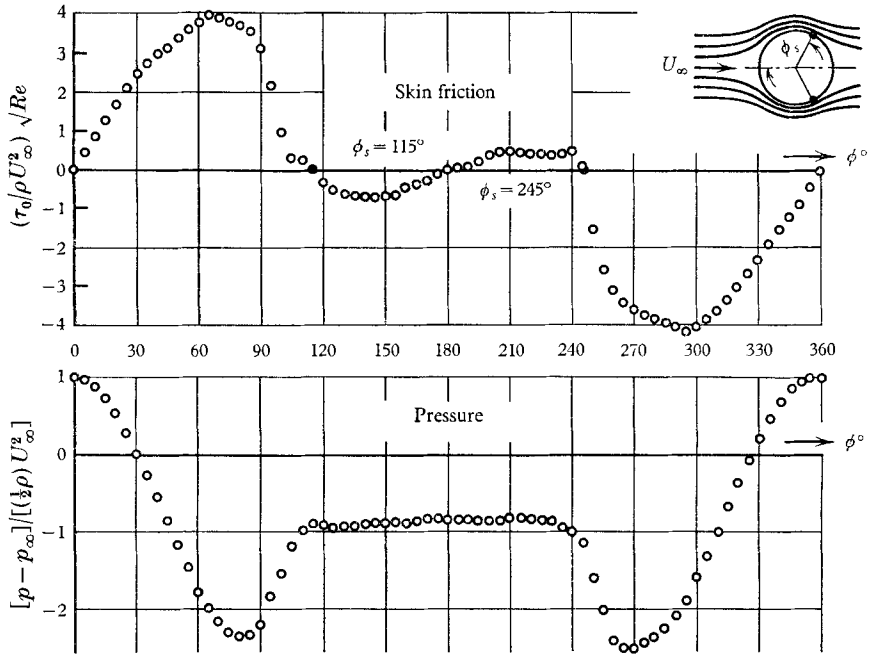

FIGURE 6. Circular cylinder: skin friction and pressure distribution. $Re = 3{\cdot}6 \times 10^6$.

surface roughness, differ in nearly all cases. For the rest, these data are not usually communicated. Therefore, one does not hope to find a satisfying agreement in a comparison of the results. Nevertheless we compared, in figure 8, our own results with those of Giedt (1951) and Fage & Falkner (1931); for they too measured the local skin friction up to $Re = 2{\cdot}1 \times 10^5$. At $Re = 10^5$ the results agree rather well except our own pressure distribution in the region of $\phi = 70°$. The comparison at $Re = 2{\cdot}1 \times 10^5$ shows that Giedt as well as Fage & Falkner measured the beginning of the separation bubble, while in our case a pronounced laminar separation occurs. This fact seems to be due to the turbulence level. Giedt and Fage & Falkner used a Stanton tube for the determination of the skin friction. Therefore they were not able to measure in the region of the recirculation.

4.2. *Position of the separation point*

The τ_0-curves crossing the zero line indicate the geometrical position of the separation. In figure 10 the position of the separation points is plotted as a function of the Reynolds number. The diagram allows one to distinguish three

flow régimes: the subcritical, the critical and the supercritical. The sudden rise from the subcritical to the critical flow at $Re = 3 \times 10^5$ is obvious. The separation point shifts from $\phi = 95°$ to $\phi = 140°$. The vanishing of the separation bubble at $Re = 1{\cdot}5 \times 10^6$ indicates that the supercritical state of flow is reached. The separation point moves in the direction of the frontal stagnation point. The

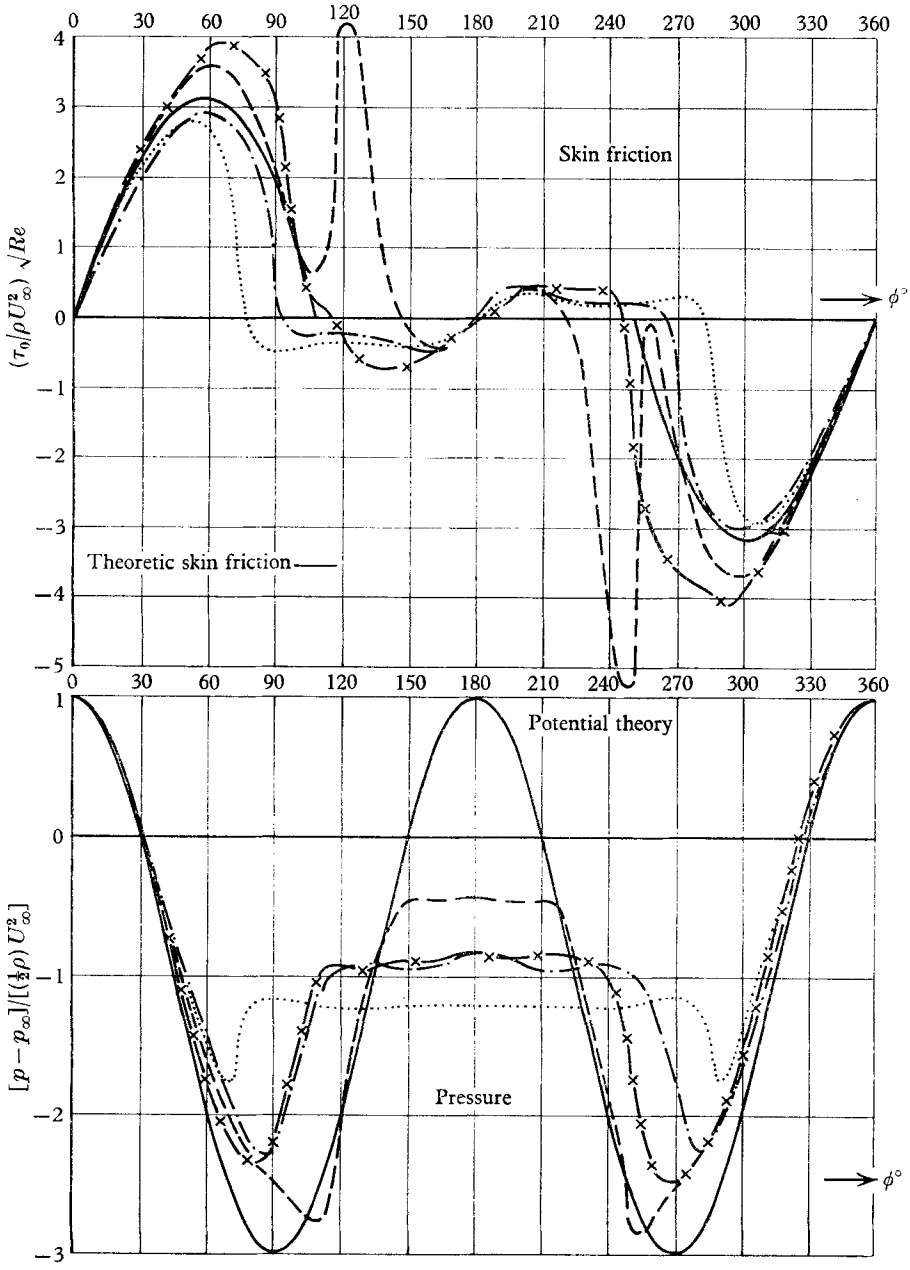

FIGURE 7. Circular cylinder: comparison of the skin friction and pressure distribution at various Reynolds numbers. . . . , $Re = 1{\cdot}0 \times 10^5$; —·—, $Re = 2{\cdot}6 \times 10^5$; ——, $Re = 8{\cdot}5 \times 10^5$; — × —, $Re = 3{\cdot}6 \times 10^6$.

separation occurs now in the range of $115° < \phi < 120°$. In the subcritical region the minimum of the separation angle at $Re = 1{\cdot}5 \times 10^5$ is remarkable. Here the lowest values of $\phi = 72°$ have been measured. This minimum indicates the beginning of the decreasing of the total drag coefficient C_D.

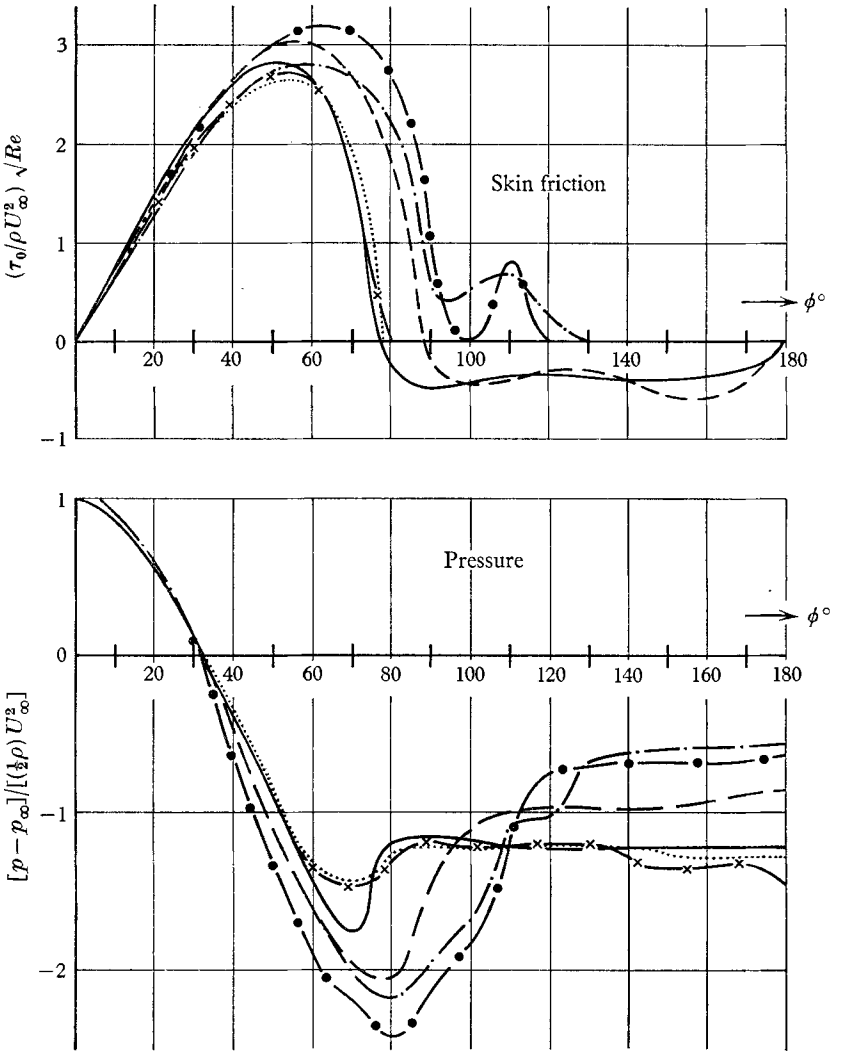

FIGURE 8. Circular cylinder: skin friction and pressure distribution, comparison with other authors. $Re = 10^5$: ——, own values; —×—, Giedt (1951); . . . ., Fage & Falkner (1931). $Re = 2{\cdot}1 \times 10^5$: ——, own values; —●—, Giedt (1951); —·—, Fage & Falkner (1931).

4.3. *Total drag coefficient*

By means of the measured pressure and skin friction distribution the total drag coefficient C_D can be calculated by an integration around the tube

$$C_D = \frac{D}{(\frac{1}{2}\rho)U_\infty^2\, dL}.$$

In figure 9 the results are plotted for two ratios of length to diameter L/d. It must be expected that there is an effect of the span-diameter ratio. The scattering of the results, however, does not allow one to outline the systematic influence. The recent investigations of Morsbach (1967) show that, in the sub-

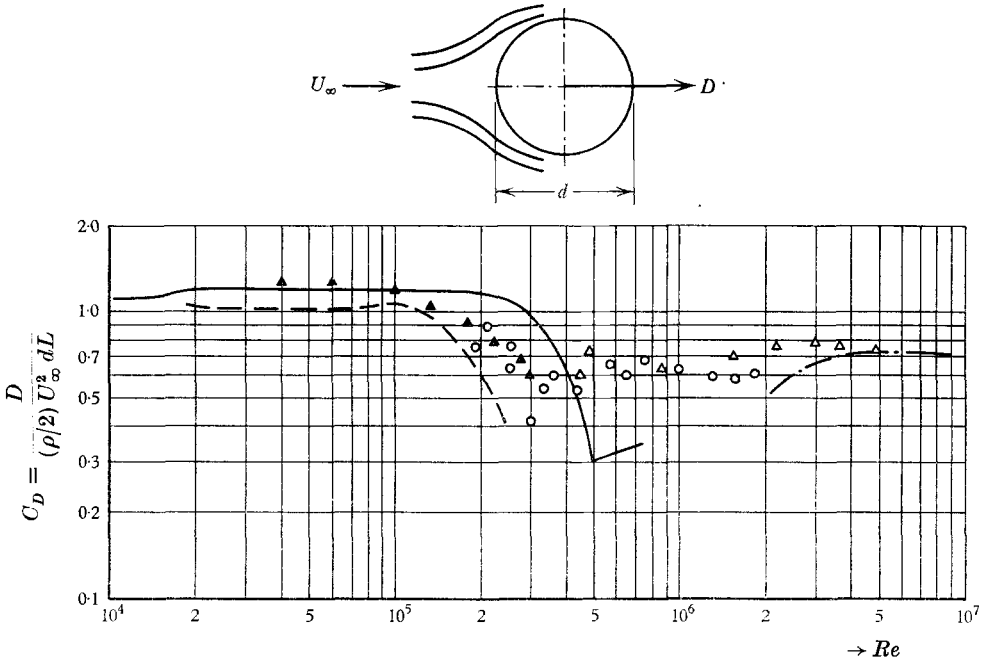

FIGURE 9. Circular cylinder: total drag coefficient as a function of the Reynolds number. ——, Wieselsberger (1923); ——, Fage & Warsap (1930); —·—, Roshko (1961); ▲, L/d = 3·33 ND channel; △, L/d = 3·33 HD channel; ○, L/d = 6·66 HD channel.

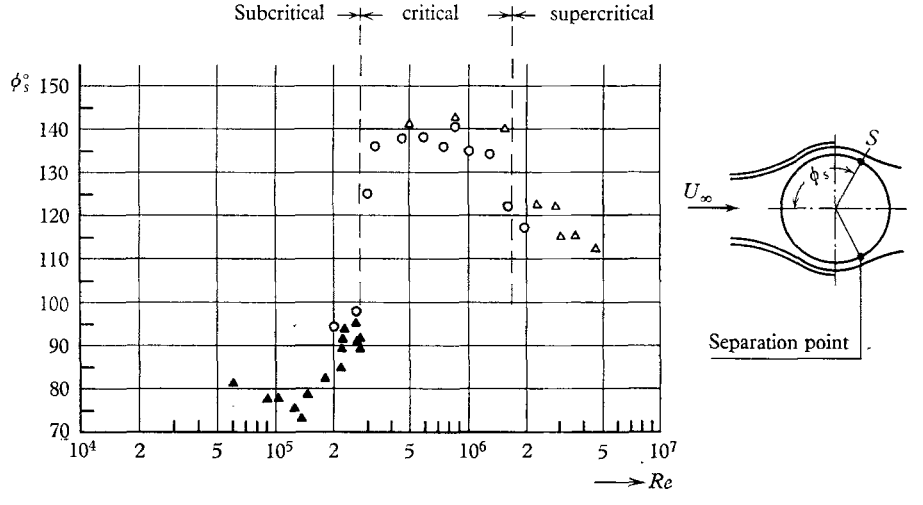

FIGURE 10. Circular cylinder: position of the separation point as a function of the Reynolds number. ▲, L/d = 3·33 ND channel; △, L/d = 3·33 HD channel; ○, L/d = 6·66 HD channel.

critical state of flow, there is no influence of the span-diameter ratio. In the critical flow, however, an effect was observed. For small values of L/d ($L/d < 3{\cdot}0$) the influence was considerable, while in the case of $L/d = 5$ the flow at the middle section of the cylinder was no longer influenced by the walls.

Concerning the investigations of Wieselsberger (1923) and Roshko (1961), as well as those of Fage & Warsap (1930), the turbulence level has, unfortunately, not been communicated. An increasing turbulence level effects a decrease of the critical Reynolds number. Therefore it may be supposed that Wieselsberger measured at a lower, Fage & Warsap at a higher turbulence level than we did ($Tu = 0{\cdot}7\,\%$). This assumption implies that the surfaces of the cylinders were polished in all cases.

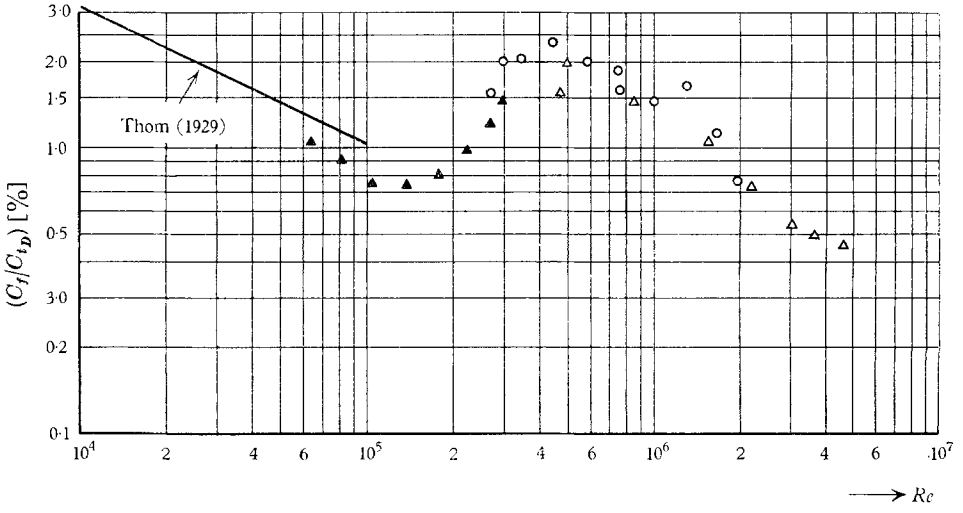

FIGURE 11. Circular cylinder: rate of the friction coefficient with respect to the total drag coefficient. ▲, $L/d = 3{\cdot}33$ ND channel; △, $L/d = 3{\cdot}33$ HD channel; ○, $L/d = 6{\cdot}66$ HD channel.

Finally it must be noticed that no correction for the blockage ratio d/H, where H is the channel width, was made. This correction was omitted, in order to avoid the measurements being subjected to a theory, which may not be correct.

4.4. *Friction forces*

The total drag of a cylinder is composed additively of pressure forces and friction forces. Thus the drag coefficient can be written

$$C_D = C_p + C_f.$$

Figure 11 presents the percentage of friction referred to the total drag as a function of the Reynolds number. In the subcritical region our own values nearly join those of Thom (1929) obtained in a semi-theoretic way. The results published by Schiller & Linke (1933) are of the same order. It is suggested that Thom's values are a little too large, because he made an addition of 4 % for the rear, while a reduction would be obvious with respect to the observed recircula-

tion. The results of Schiller & Linke (1933) may be regarded to be of moderate accuracy because of the method used. Their results are the difference of two large terms of nearly the same order. The rate of friction was obtained by a comparison of the directly measured forces with the integration of the local pressure around the cylinder. In our case, however, the experimental skin friction has been integrated.

By means of figure 11 we find that the friction forces are nearly unimportant with respect to the quantity of the total drag. Nevertheless they influence the flow causally by effecting the separation of the boundary layer.

5. Discussion of the results

For the measurements of the pressure and the skin friction, as well as for the calculations, the flow around the cylinder was regarded to be of the steady type. This is not true exactly because of the alternating eddy separation, which causes an oscillation of the boundary layer up to the stagnation point. Therefore the measured local values are temporal mean values. The averaging process is unknown, because it depends on the co-operation of the probe, mains and measuring instruments. However, an eventual systematic error is so small that there is no discrepancy between the mean pressure distribution and the corresponding mean skin friction distribution. The application of the skin friction probe leads to the question, whether the edge, which can be regarded as a discrete roughness element, influences the flow. According to the measurements of Fage & Preston (1941) the transition from laminar to turbulent boundary layer in a flow without pressure gradient occurs at a critical dimensionless roughness height $y^* = 20$,

$$y^* = \frac{(\tau_0/\rho)^{\frac{1}{2}} h\rho}{\eta}.$$

In our own atmospherical experiments this value y^* was always lower than 4·5. Concerning the investigations in the HD channel, the largest value $y^* = 40$ was reached at the highest Reynolds number in the position of the maximum skin friction; this means that a premature transition may be caused by the probe. This fact seemed to be confirmed when applying Kraemer's (1961) criterion:

$$Re_{\text{crit}} = \frac{Uh\rho}{\eta} \leqslant 900,$$

because the obtained maximum critical Reynolds number was $Re_{\text{crit}} = 1800$.

In order to get a decision from the experiment, we measured the pressure distribution for control by means of an additional pressure hole, drilled at a distance of 30 mm from the skin friction probe on the same generator. Within the accuracy no deviation of the pressure distribution could be observed. From this result it was concluded that the probe had not yet influenced the flow. It is suggested that the reason for this discrepancy is the intensive pressure gradient.

The pressure and the skin friction were measured around the circumference of the cylinder from $\phi = 0°$ to $\phi = 360°$. Thus it is noticed that sometimes

there is an unsymmetrical flow. The asymmetry has been observed independent of different length to diameter ratios. The flow around the cylinder is sensitive in such a way that the smallest disturbances of the flow at the entrance of the test section are suggested to cause the asymmetry.

At high Reynolds numbers the boundary-layer changes from the laminar to the turbulent state. The skin friction probe was calibrated in the laminar boundary layer only. Therefore we cannot be sure that the values of the turbulent boundary layer are reliable. In this sense the investigations of Bradshaw & Gregory (1959) are interesting. The authors analyse different methods of measuring local skin friction. One of the methods used by them in their experiments is that of the Stanton tube, which, concerning the principle, comes closest to our procedure. They demonstrate, for a flow without, respectively with very small pressure gradient, that a Stanton tube calibrated in a laminar boundary layer and working in a turbulent flow yields values of wall shear stresses which are too low. From these results it may be concluded that our turbulent skin friction may be too small. Unfortunately the results of Bradshaw & Gregory cannot be evaluated for our case, because the influence of the considerable pressure gradient is unknown.

The author is indebted to Dr H. Grosse, director of the 'Institut für Reaktorbauelemente der Kernforschungsanlage Jülich' who made this investigation possible. He is also grateful to all people whose co-operation he was dependent on, especially to Mr H. Gillessen, Mr F. Hoffmanns, Mr H. Reger, Mr W. Schmidt and Mr G. Türk for their assistance in preparing and performing the experiments.

REFERENCES

Bradshaw, P. & Gregory, N. 1959 The determination of local turbulent skin friction from observations in the viscous sub-layer. *Aero. Res. Counc. Lond. R. & M.* no. 3202.

Fage, A. & Falkner, V. M. 1931 Further experiments on the flow around a circular cylinder. *Aero. Res. Counc. Lond. R. & M.* no. 1369.

Fage, A. & Preston, J. H. 1941. On transition from laminar to turbulent flow in the boundary layer. *Proc. Roy. Soc.* A **178**, 201–27.

Fage, A. & Warsap, J. H. 1930 The effect of turbulence and surface roughness on the drag of a circular cylinder. *Aero. Res. Counc. Lond. R. & M.* no. 1283.

Giedt, W. H. 1951 Effects of turbulence level of incident airstream on local heat transfer and skin friction on a cylinder. *J. Aero. Sci.* **8**, 725–30.

Grosse, H. & Scholz, F. 1965 *Der Hochdruck-Gaskanal. Kerntechnik*, Heft 4. München: Thiemig.

Konstantinov, N. I. & Dragnysh, G. L. 1955 The measurement of friction stress on a surface. *D.S.I.R.* RTS 1499 (1960).

Kraemer, K. 1961 Über die Wirkung von Stolperdrähten auf den Grenzschichtumschlag. *Z. Flugwiss*, **9**, 20–7.

Morsbach, M. 1967 Über die Bedingungen für eine Wirbelstraßenbildung hinter Kreiszylindern. Dissertation T. H. Aachen (1967).

Rechenberg, I. 1962 Zur Messung der turbulenten Wandreibung mit dem Prestonrohr. *Jahrbuch der Wissenschaftlichen Gesellschaft für Luft- und Raum-fahrt* e.V. (WGLR), 151–9.

RECHENBERG, I. 1963 Messung der turbulenten Wandschubspannung. *Z. Flugwiss*, **11**, 429–38.

ROSHKO, A. 1961 Experiments of the flow past a circular cylinder at very high Reynolds number. *J. Fluid Mech.* **10**, 345–56.

SCHILLER, L. & LINKE, W. 1933 Druck- und Reibungswiderstand eines Zylinders bei Reynolds' schen Zahlen 5000 bis 40000. *Z. Flugtech. Motorluftschiff.* **24**, Heft 7, 193–8.

SCHLICHTING, H. 1955 *Boundary layer theory*. Oxford: Pergamon.

THOM, A. 1929 An investigation of fluid flow in two dimensions. *Aero. Res. Counc. Lond. R. & M.* no. 1194.

WIESELSBERGER, C. 1923 Versuche über den Widerstand gerundeter und kantiger Körper. *Ergebnisse A V A Göttingen II Lieferung* (1923).